

Research Article

ISOTHERMAL CRYSTALLISATION KINETICS OF MICROBIAL POLY(3-HYDROXYBUTYRATE-CO-3-HYDROXYHEXANOATE)

YOGA SUGAMA SALIM^{1,2}, CHIN HAN CHAN^{2,*}, KUMAR SUDESH³, SENG NEON GAN¹

¹ Department of Chemistry, Universiti Malaya, 50603 Kuala Lumpur, Malaysia, ² Faculty of Applied Sciences, Universiti Teknologi MARA, 40450 Shah Alam, Malaysia, ³ School of Biological Sciences, Universiti Sains Malaysia, 11700 Penang, Malaysia.
Email: cchan@salam.uitm.edu.my

Received: 05 Feb 2014 Revised and Accepted: 03 Apr 2014

ABSTRACT

Polyhydroxyalkanoates (PHA), a class of microbial polyesters produced from fermentation, is of interest for scientists and environmentalists due to its wide-ranged combinations of monomers, biodegradability and biocompatibility properties. In this study, efforts were made to understand the kinetics of isothermal crystallisation of PHA containing 3 mol% of 3-hydroxyhexanoate (3HHx) co-monomer [P(3HB-co-3 mol% 3HHx)]. Avrami model is used to describe the kinetics of the isothermal crystallisation. Besides, we discuss crystallinity, equilibrium melting temperature, kinetics of isothermal crystallisation and activation energy of isothermal crystallisation of P(3HB-co-3 mol% 3HHx). The average crystallinity of P(3HB-co-3 mol% 3HHx) is found to be 42.5% when it is isothermally crystallised from 121-127 °C. Meanwhile, the equilibrium melting temperature of P(3HB-co-3 mol% 3HHx) (T_m^0) is 183 °C, which is in good agreement to the T_m^0 s of various PHA reported in the literature. Half-time of crystallisation ($t_{0.5}$) increases exponentially with temperature. Correspondingly, overall rate of isothermal crystallisation ($K^{1/n}$) decreases with temperature. The isotherms of crystallisation exhibit sigmoid dependence on time, and they gradually shift toward longer crystallisation times with increasing crystallisation temperature. Kinetic data are compared with data for other alkanates and copolymers with them.

Keywords: poly(3-hydroxybutyrate-co-3-hydroxyhexanoate), Isothermal crystallisation, Avrami

INTRODUCTION

As the world demand of environmentally friendly material increases, interest in biodegradable polymers from renewable resources also increases. Natural polyesters, namely polyhydroxyalkanoates (PHA), are by far one of the most attractive polymers owing to their environment-friendly features such as biodegradabilities [1, 2] and biocompatibilities [3, 4]. The best known PHA, poly(3-hydroxybutyrate) [P(3HB)], possesses high crystallinity ($X_c=55-65\%$) [5] and is thermally unstable [6, 7]. To overcome this, random copolymers such as poly(3-hydroxybutyrate-co-4-hydroxybutyrate) [P(3HB-co-4HB)], poly(3-hydroxybutyrate-co-3-hydroxyvalerate) [P(3HB-co-3HV)] and poly(3-hydroxybutyrate-co-3-hydroxyhexanoate) [P(3HB-co-3HHx)] are often introduced. The copolymers range of P(3HB-co-3HHx), in mol%, can be tailor-made using recombinant biotechnology as well as the choice of carbon substrate used in the fermentation process [8, 9]. This semicrystalline polymer has wider thermal processing window, with lower melting temperature and longer elongation at break, compared to P(3HB). All the PHA mentioned above is of importance in the field of pharmaceutical and biomedical industry, for example as biomedical scaffolding and surgical materials [10, 11], as well as drug delivery devices [12-14]. Before PHA is readily used, in most cases, it must first be processed using plastic processing machineries such as mixers, extruders, injection moulding. Thus, it is vital to understand the equilibrium concepts that form the basis for the understanding of the aspects of crystallisation process [15]. As a matter of fact, the mechanical properties of a semicrystalline polymer are influenced by the molecular morphology, which in turn is governed by the crystallisation kinetics. There have been numerous investigations reported on the isothermal and non-isothermal crystallisation of P(3HB-co-3HHx) using Avrami approach [16-18]. Chen and coworkers (2005) studied the isothermal crystallisation kinetics at low crystallisation temperature ($T_c = 48-60$ °C) and showed that the activation energy of isothermal crystallisation (ΔE) of PHA increases with increasing 3HHx contents. As a consequence, the overall isothermal crystallisation rate ($K^{1/n}$) descends with increasing crystallisation temperature and 3HHx content, as reported by Cai and Qiu (2009). They demonstrated that isothermal crystallisation kinetics of P(3HB-co-15 mol% 3HHx) obey Avrami model at early transformation range of crystallisation and display the Avrami exponents (n) ranging between 2.4 and 3.2.

In this work, we employ the Avrami model to analyse isothermal crystallisation kinetics of P(3HB-co-3HHx) by differential scanning calorimeter (DSC) with low 3HHx content (3 mol%). Unlike the 3HV monomers which cocrystallises with 3HB (a phenomenon termed isodimorphism), the bulky 3HHx monomer is excluded from the 3HB crystal, resulting in significant changes in physical properties even at small amount of 3HHx. We encountered many practical problems for the area of integration of relative crystallinity developed during isothermal crystallisation from the DSC exotherms of P(3HB-co-3HHx). Practical guidelines on how to reduce the error of peak area integration for DSC isothermal crystallisation will be addressed. Besides, crystallinity, melting behaviour, kinetics of isothermal crystallisation and activation energy of isothermal crystallisation are highlighted for P(3HB-co-3 mol% 3HHx).

MATERIALS AND METHODS

Materials

P(3HB-co-3 mol% 3HHx) was obtained through biosynthesis. Chloroform (CHCl_3) and methanol (CH_3OH) were commercially available in American Chemical Standard (ACS) grade (Merck KGaA, Darmstadt, Germany) and used without further purification, unless stated.

Biosynthesis of P(3HB-co-3 mol% 3HHx)

Biosynthesis of P(3HB-co-3 mol% 3HHx) was carried out using *C. necator* PHB⁻⁴ transformant harboring the PHA synthase enzyme of *Aeromonas caviae* [19]. The *C. necator* PHB⁻⁴ was grown in 250 mL conical flasks containing nutrient rich (NR) broth under aerobic conditions at 30 °C until the optical density reached 4.5-5. The NR medium was then transferred into mineral salts medium formulation according to Doi *et al.*, 1990 [20]. The cultivated cells after 36 h were harvested by centrifugation, washed with distilled water and lyophilised (freeze-drying). Pure P(3HB-co-3 mol% 3HHx) was obtained by dissolution in CHCl_3 at 50 °C and precipitated in ice-cold CH_3OH before drying in fume hood and vacuum drying in Memmert Oven at 50 °C for 24 h. To determine the PHA content and monomer composition, lyophilised cells were subjected to methanolysis in the presence of 15% (v/v) sulphuric acid and 85% (v/v) methanol, before the analysis using gas

chromatography [21]. It was shown that the P(3HB-co-3 mol% 3HHx) produced from the biosynthesis contained 3 mol% of 3HHx. The weight-average (M_w) and number-average (M_n) molecular weight of neat P(3HB-co-3 mol% 3HHx) was estimated by GPC at 40 °C using an Agilent 1200 GPC (Agilent, USA) coupled with refractive index detector and Waters Styragel columns (HR 3 and HR 5E). CHCl₃ HPLC grade (Fisher Scientific, UK) was used as eluent at flow rate of 0.8 mL min⁻¹ and solvent with sample concentration of 1.0 mg mL⁻¹. Polystyrene standards (Sigma-Aldrich, USA) ($M_w = 70,000$ to 1,000,000 g mol⁻¹) with narrow polydispersity were used to prepare the calibration curve. From the GPC analysis, P(3HB-co-3 mol% 3HHx) had M_n of 4.0×10^5 g mol⁻¹, M_w of 7.4×10^5 g mol⁻¹ and polydispersity of 1.8.

DSC measurement

An exact mass of 3.00-7.00 mg P(3HB-co-3 mol% 3HHx) samples were encapsulated in standard DSC aluminum pans (Perkin Elmer, USA). Thermal analysis of bacterially synthesised P(3HB-co-3 mol% 3HHx) was carried out using TA Instruments DSC Q200 (USA). High purity indium under high-purity (purity: 99.9995%) nitrogen atmosphere (flow rate: 50 mL min⁻¹) was used for Tzero calibrations (cell constant and heat capacity) and isothermal study. The isothermal crystallisation was performed by the following thermal procedures (a) samples were heated from 30 °C to 175 °C at a rate of 10 °C min⁻¹ for 3 min and rapidly cooled to a predetermined crystallisation temperature, T_c (121-127 °C), until complete crystallisation where no significant change of heat flow was seen as a function of time. The $t_{0.5}$ can be estimated using horizontal baseline integration, which will be discussed later in Section 4. Once $t_{0.5}$ was obtained, the following step was employed to extract the kinetics information: (b) samples were heated from 30 °C to 175 °C at a rate of 10 °C min⁻¹ for 3 min and rapidly cooled to several T_c s and isothermal for five $t_{0.5}$ s (to ensure same extent of crystallisation for all samples), then the samples were heated again to 175 °C at a rate of 10 °C min⁻¹ to determine the melting point of corresponding polymer crystals. For each experiment, a fresh sample was prepared to minimise the influence of molecular weight degradation on the crystallisation behaviour. As mentioned before, PHA is known to thermally degrade at and above its melting temperature [6, 7]. Under identical conditions, a single DSC experiment at $T_c = \text{const}$ is used for each regression calculation. The errors were estimated using regression analysis based on 2-tailed student *t*-test at 95% confidence level.

RESULTS AND DISCUSSION

Crystallinity

Crystallinity (X^*) of P(3HB-co-3 mol% 3HHx) is estimated according to Eq. (1).

$$X^* = \frac{\Delta H_m}{\Delta H_{\text{ref}}} \quad (1)$$

where, ΔH_m is the melting enthalpy of P(3HB-co-3 mol% 3HHx) after being isothermal crystallised for five $t_{0.5}$ s at preselected T_c . ΔH_{ref} is the theoretical melting enthalpy of 100% crystalline P(3HB) (146 J g⁻¹) according to Barham *et al.*, 1984 [5]. After the PHA sample was isothermally crystallised at preselected T_c for a period of five $t_{0.5}$ s, samples were heated with a rate of 10 °C min⁻¹ for determination of melting enthalpies (ΔH_m). The corresponding normalised ΔH_m , with respect to sample mass, was plotted against T_c (shown in Fig. 1). It was evident that ΔH_m of P(3HB-co-3 mol% 3HHx) remained constant in the temperature range of crystallisation. The average X^* after Eq. (1) of P(3HB-co-3 mol% 3HHx) was 42.5% with reference to 100% crystalline material of P(3HB). It was shown that incorporation of 3 mol% of 3HHx reduced the crystallinity by approximately 10-20% compared to that of P(3HB).

Melting behaviour of P(3HB-co-3 mol% 3HHx)

In general, melting and crystallisation temperatures of polymers are not in equilibrium state; the crystallisation rate is so slow at temperature close to the T_m^0 that it takes years to crystallise. Hence,

crystallisation of P(3HB-co-3 mol% 3HHx) can only proceed at a temperature below T_m^0 . Quantity of P(3HB-co-3 mol% 3HHx) was determined experimentally by step-wise annealing procedure after Hoffman-Weeks [22]. The Hoffman-Weeks equation is as follow

$$T_m = (1/\gamma) T_c + T_m^0 (1 - 1/\gamma) \quad (2)$$

where, T_m = melting temperature and T_c = crystallisation temperature, $1/\gamma$ = stability parameter from ratio of final to initial lamellar thickness, which is affected by crystal size and perfection. From the plot of T_m versus T_c , extrapolation of experimental data to the intersection of $T_m = T_c$ yields T_m^0 .

The procedure of Hoffman-Weeks served for determination of equilibrium melting temperature. Accordingly, we expect linear variation of melting temperature with crystallisation temperature

leading to T_m^0 at $T_m = T_c$. Hoffman-Weeks plot for melting temperature of P(3HB-co-3 mol% 3HHx) as function of crystallisation temperature is shown in Fig. 2. Linear relationship was observed for P(3HB-co-3 mol% 3HHx) within selected crystallisation temperature range. The estimated T_m^0 of P(3HB-co-3 mol% 3HHx) was 183 ± 7 °C, according to Eq. (2), and the value of $1/\gamma$ (slope) was 0.44. When $1/\gamma$ is close to zero, it showed crystallisation without chain folding or development of extended-chain crystals. The T_m^0 s of P(3HB), P(3HB-co-7 mol% 3HHx), P(3HB-co-10 mol% 3HHx) and P(3HB-co-18 mol% 3HHx) reported in the literature are 197 °C [5], 167 ± 6 °C [17], 164 ± 4 °C [17], and 161 ± 4 °C [17], respectively. The trend is in agreement to our results, with 3 mol% 3HHx.

Kinetics of isothermal crystallisation

Avrami equation [15] used to describe the kinetics of the isothermal crystallisation of P(3HB-co-3 mol% 3HHx) is given as follow:

$$X(t) = 1 - \exp[-K^{1/n}(t - t_0)^n] \quad (3)$$

where, $X(t)$ is relative crystallinity at time t ; t_0 is an induction period; $K^{1/n}$ is an overall rate of crystallisation (min⁻¹); and n is the Avrami exponent that depends on the type of nucleation and geometry of growing polymer crystals. Rearrangement of Eq. (3) arrives at Eq. (4):

$$\lg[-\ln(1 - X)] = \lg K^{1/n} + n \lg(t - t_0) \quad (4)$$

$K^{1/n}$ and n can be extracted from the intercept and the slope of the Avrami plot in Eq. (4).

The prime requirement of Avrami model is the ability of the spherulites of P(3HB-co-3 mol% 3HHx) to grow in a free space. Besides, Avrami equation is usually only valid at low degree of conversion as long as the impingement of the P(3HB-co-3 mol% 3HHx) spherulites has yet to take place. The exothermic crystallisation curves of P(3HB-co-3 mol% 3HHx) at various crystallisation temperatures were shown in Fig. 3. It became obvious that increase of crystallisation temperature led to longer crystallisation time. In ideal condition, the crystallisation peaks referred to flat baseline as indicated by the dashed curve in Fig. 3, e.g. P(3HB-co-3 mol% 3HHx) isothermally crystallised at 127 °C; however in many cases, the starting and end points did not fall on the flat baseline, e.g. PHA isothermally crystallised at $T_c=121-123$ °C. Lorenzo *et al.*, 2007 [23] state that choice of induction time (t_0) and baseline of exothermic peaks is important for estimation of $X(t)$. In our study, we employed the projection of horizontal baseline, as shown in Fig. 4(b), by extrapolation from the end point of crystallisation curves, as proposed by Hay and Mill [24]. This technique has been proven to have a minimal systematic error at various crystallisation temperatures compared to a straight line

integration shown in Fig. 4(a). By using the projection of horizontal baseline, $t_{0.5}$ for P(3HB-co-3 mol% 3HHx) crystallised at 127 °C, 123 °C and 121 °C were 11.6 min, 4.9 min, and 3.5 min, respectively. When straight line integration was applied, there was an error in the area of integration e.g. around 13-18 min for P(3HB-co-3 mol% 3HHx) crystallised at 123 °C; thus the calculated $t_{0.5}$ deviated around 6% (5.2 min) from that using horizontal baseline method shown later in Fig. 5. The crystallisation enthalpy, ΔH_c , of isothermal crystallisation of P(3HB-co-3 mol% 3HHx) was also affected by the types of integration. For example, the technique of horizontal baseline showed a ΔH_c of 61.3 J g⁻¹, while the straight line integration showed a ΔH_c of 51.0 J g⁻¹ when P(3HB-co-3 mol% 3HHx) was isothermally crystallised at 123 °C. The former integration showed a close value to that its ΔH_m (the melting enthalpy after the samples was isothermally crystallised at 123 °C for five $t_{0.5}$ s), with a relative error of 0.3%, while the latter integration showed a relative error of 16.5% from ΔH_m . In short, it is of paramount importance to select a suitable baseline to integrate the isothermal crystallisation exotherm in order to obtain reliable results for the crystallisation kinetics.

As previously mentioned, an important parameter associated with crystallisable component is $t_{0.5}$, which is defined as the time at which the extent of crystallisation is 50% complete. Fig. 5 shows the plot of $t_{0.5}$ versus T_c for P(3HB-co-3 mol% 3HHx) at various T_c s. By lowering the T_c from 127 to 121 °C, it took shorter time for P(3HB-co-3 mol% 3HHx) to crystallise. The plot of $t_{0.5}$ versus T_c yielded exponential increase for P(3HB-co-3 mol% 3HHx). The smaller value of $t_{0.5}$ indicates faster overall crystallisation rate. The Avrami plot of P(3HB-co-3 mol% 3HHx) crystallised at various T_c s is shown in Fig. 6. Although the linearity (straight line) was not observed over the entire transformation range in P(3HB-co-3 mol% 3HHx), a very good agreement ($r^2=0.999$) to Avrami is found in a certain range of time with up to 80% of the degree of conversion. This was due to the secondary crystallisation that took place after impingement. Again, the quantity $K^{1/n}$ can be obtained from intercept of the plot of $\log[-\ln(1-X)]$ versus $\log(t-t_0)$ while the slope represents Avrami exponent (n), as shown in Eq. (4). It was shown that the $K^{1/n}$ reduced exponentially with increasing crystallisation temperature (Fig. 7). This trend was in good agreement to the results obtained from the plot of T_c versus $t_{0.5}$ (Fig. 5). The experimental values of n vary between 2.46 ± 0.04 and 3.28 ± 0.04 . Our results resembled to that of the study by Chen *et al.* [16]. They found the Avrami index of P(3HB-co-3HHx) containing 15 mol% 3HHx varies from 2.6 to 2.8. Another work by Cai and Qiu (2009) also shows the Avrami index varies between 2.4 and 3.2 for P(3HB-co-3HHx) containing 7, 10 and 18 mol% 3HHx [17]. The crystallisation mechanism of P(3HB-co-3HHx) may

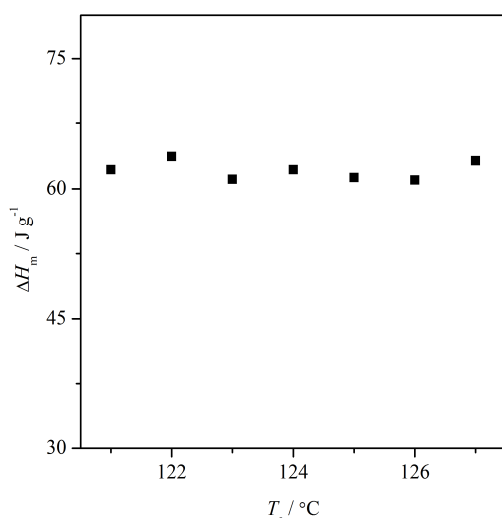


Fig. 1: Plot of ΔH_m against crystallisation temperature for P(3HB-co-3 mol% 3HHx)

not be easily resolved due to the Avrami index is a combination characteristic of nucleation and growth. The explanation on the growth dimension and nucleation is rather limited without data from optical micrographs. All the Avrami parameters mentioned are summarised in Table 1.

Activation energy of isothermal crystallisation

Arrhenius-like relationship [22] for the rate of isothermal crystallisation can be described as

$$\frac{1}{t_{0.5}} = \frac{1}{\tau} \exp\left[-\frac{E}{k_b T_c}\right] \quad (6)$$

where, E is defined as the energy of formation of a lamella, which is

inversely proportional to undercooling, $\Delta T_c \equiv T_m^0 - T_c$, k_b is a Boltzmann constant and τ is a constant that does not depend on

temperature. Hence, the exponent in (6) is $B T_m^0 / (T_c \Delta T_c)$, with RB being the activation energy. In linear approximation in ΔT_c and

$\Delta T_c / T_m^0 \approx \text{const}$, it follows:

$$\frac{1}{t_{0.5}} = \frac{1}{\tau} \exp\left[-\frac{B}{\left(1 - \frac{\Delta T_c}{T_m^0}\right) \Delta T_c}\right] \quad (7)$$

Fig. 8 shows a semilogarithmic plot according to Eq. (7). The Arrhenius activation energy of isothermal crystallisation is associated to the overall process of crystallisation of P(3HB-co-3 mol% 3HHx). From our data, it was shown that the average of

$\Delta T_c / T_m^0$ was almost constant, therefore the activation energy was calculated to be 3.9 kJ mol⁻¹. By employing the data of Chan *et al.* [25] and Chen *et al.* [16] to Arrhenius approach, the calculated activation energy of P(3HB) and P(3HB-co-15 mol% 3HHx) was found to be 5.2 kJ mol⁻¹ and 0.5 kJ mol⁻¹, respectively. Further data analysis obtained by Cai and Qiu (2009) suggests that the activation energy of P(3HB-co-7 mol% 3HHx), P(3HB-co-10 mol% 3HHx) and P(3HB-co-18 mol% 3HHx) is 1.3 kJ mol⁻¹, 1.1 kJ mol⁻¹, and 0.6 kJ mol⁻¹, respectively [17]. The increase of flexible chains in the PHA reduced the activation energy, which was responsible for the energy required to crystallise. All the activation energies of isothermal crystallisation are summarised in Table 2.

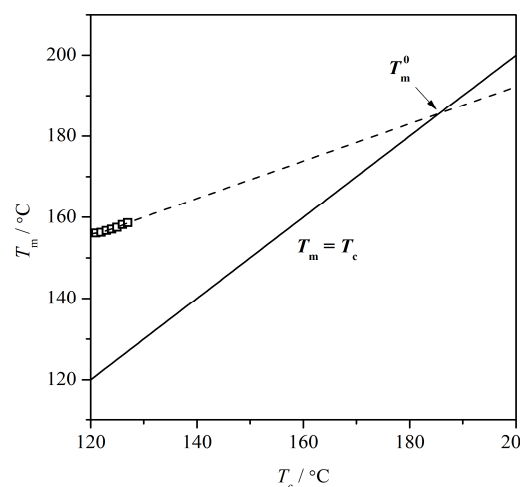


Fig. 2: Extrapolation of T_m^0 from the melting temperature as a function of isothermal crystallisation of P(3HB-co-3 mol% 3HHx) (dashed curve is for visual aid of extrapolation)

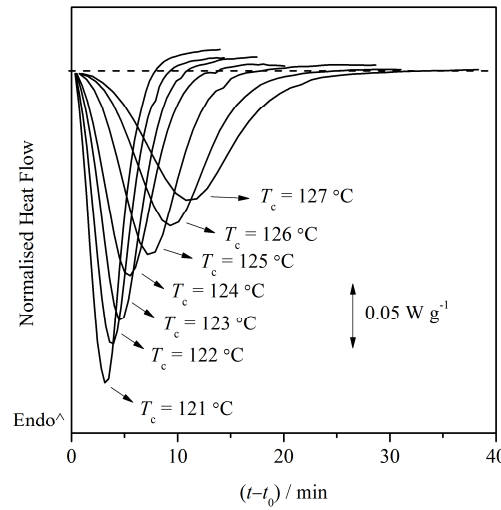


Fig. 3: Exothermic crystallisation peaks of P(3HB-co-3 mol% 3HHx) crystallised at various T_c s (dashed curve is meant for visual aid describing an ideal case of baseline)

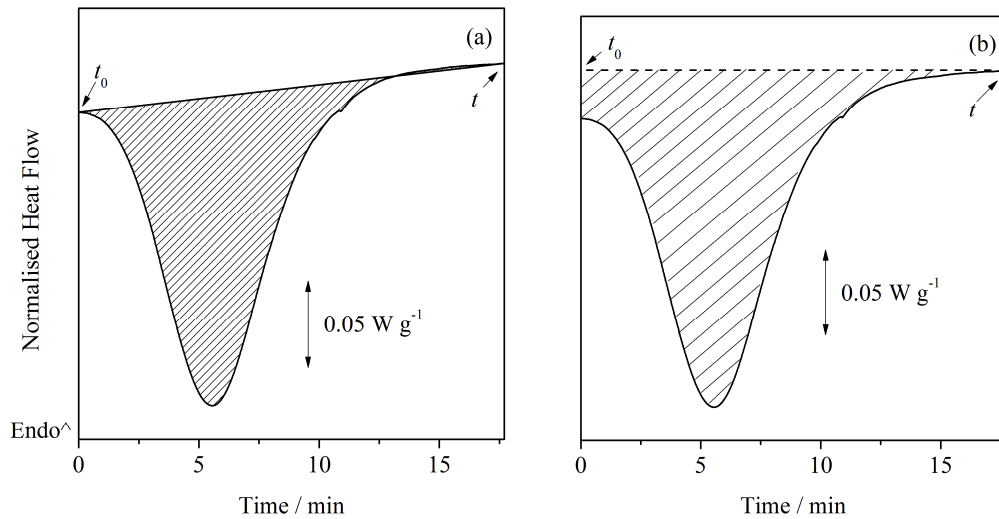


Fig. 4: Exothermic crystallisation peaks of P(3HB-co-3 mol% 3HHx) isothermally crystallised at 123 °C analysed using (a) flat line integration and (b) horizontal baseline integration

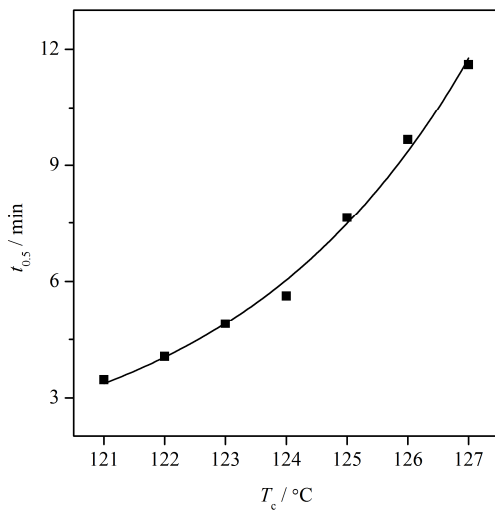


Fig. 5: Plot of $t_{0.5}$ versus T_c for P(3HB-co-3 mol% 3HHx) after isothermal crystallisation

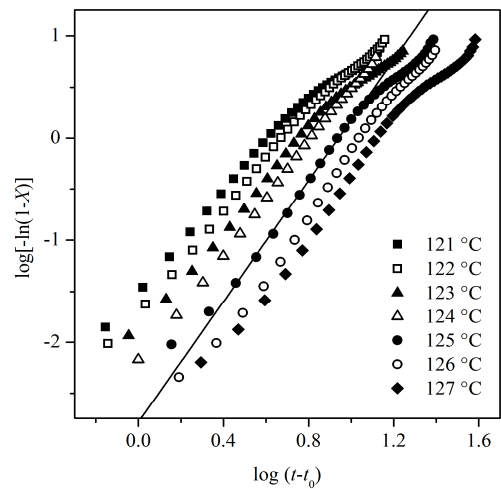


Fig. 6: Avrami plot of P(3HB-co-3 mol% 3HHx) isothermally crystallised at various crystallisation temperatures (linear curve shows the fitting that obeys Avrami model)

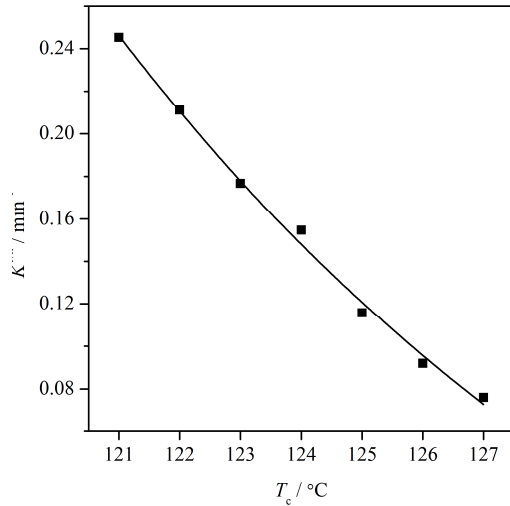


Fig. 7: Overall rate constant ($K^{1/n}$) versus crystallisation temperature (T_c) for P(3HB-co-3 mol% 3HHx)

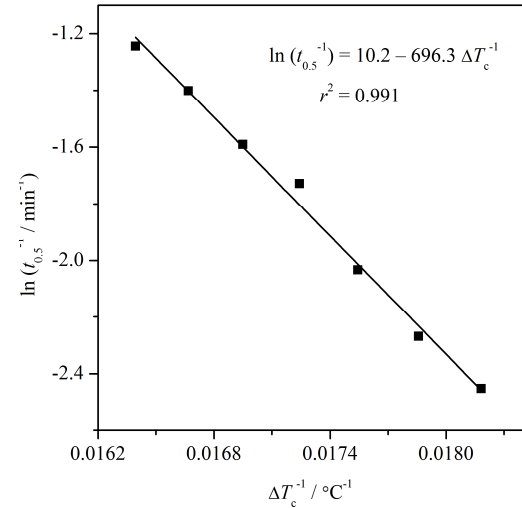


Fig. 8: Activation energy of P(3HB-co-3 mol% 3HHx) using Arrhenius-like relationship ($r^2 = 0.991$)

Table 1: Avrami parameters for the kinetics of isothermal crystallisation in P(3HB-co-3 mol% 3HHx)

T_c (°C)	t_0 (min)	$t_{0.5}$ (min)	$t_{0.5}^*$ (min)	T_m (°C)	ΔH_m (J g ⁻¹)	n	$K^{1/n} \times 10^{-4}$ (min ⁻¹)	r^2
121	21.0	3.47	3.49	156.1	62.2	2.46 ± 0.04	2453 ± 11	0.999
122	21.3	4.06	4.14	156.3	63.7	2.53 ± 0.06	2110 ± 21	0.998
123	21.4	4.91	4.88	156.7	61.1	2.56 ± 0.12	1767 ± 2	0.998
124	22.0	5.63	5.49	157.1	62.2	2.79 ± 0.05	1547 ± 13	0.999
125	21.4	7.64	8.25	157.5	61.3	3.10 ± 0.05	1157 ± 4	0.999
126	21.5	9.67	9.71	158.2	61.0	3.28 ± 0.04	920 ± 4	0.999
127	22.2	11.60	11.78	158.6	63.2	3.14 ± 0.04	761 ± 3	0.999

$$t_{0.5}^* = \left(\frac{\ln 2}{K} \right)^{1/n}$$

* calculated value, using

r^2 = correlation coefficient

Table 2: Activation energy of PHA using Hoffman's Arrhenius-like relationship

Sample	Activation energy (kJ mol ⁻¹)	r^2	Comments
P(3HB)	5.2	0.986	[25]
P(3HB-co-3 mol%-3HHx)	3.9	0.991	This study
P(3HB-co-7 mol%-3HHx)	1.3	0.997	[17]
P(3HB-co-10 mol%-3HHx)	1.1	0.993	[17]
P(3HB-co-15 mol%-3HHx)	0.5	0.939	[16]
P(3HB-co-18 mol%-3HHx)	0.6	0.992	[17]

List of symbols

Symbol	Description
$1/\gamma$	Stability parameter from ratio of final to initial lamellar thickness
τ	Constant that does not depend on temperature
ΔE	Activation energy of isothermal crystallisation
ΔH_c	Crystallisation enthalpy
ΔH_m	Melting enthalpy after isothermal crystallisation for five $t_{0.5}$
ΔH_{ref}	Theoretical melting enthalpy of 100% crystalline material
ΔT_c	Undercooling temperature
k_b	Boltzmann constant
n	Avrami exponent
t	Crystallisation time
t_0	Induction time
$t_{0.5}$	Half-time of isothermal crystallisation
E	Energy of formation of a lamella
$K^{1/n}$	Overall rate of isothermal crystallisation
T_m^0	Equilibrium melting temperature
M_n	Number average molecular weight
M_w	Weight average molecular weight
T_c	Crystallisation temperature
X^*	Relative crystallinity
$X(t)$ or X	Fraction of uncrystallizable component at time t

CONCLUSIONS

As naturally occurring biopolyesters produced inside the cells of many microorganisms, PHA has found useful applications in pharmaceutical and biomedical field. Studies on the crystallinity, melting behaviour, kinetics of isothermal and activation energy of P(3HB-co-3 mol% 3HHx) were shown for P(3HB-co-3 mol% 3HHx) in this work. The Avrami model was successfully used to describe the isothermal crystallisation of PHA with low content of 3HHx (3 mol%). The average crystallinity of P(3HB-co-3 mol% 3HHx) and the equilibrium melting temperature of P(3HB-co-3 mol% 3HHx) is 42.5% and 183 °C, respectively, when it was isothermally crystallised from 121-127 °C. The observable half-time crystallisation increases exponentially while the overall rate of isothermal crystallisation decreases exponentially with increasing crystallisation temperatures. The activation energy of isothermal crystallisation of P(3HB-co-3 mol% 3HHx) is in good agreement to that of other PHA with different mol% of 3HHx. Based on these results, a small amount of 3HHx can result in significant changes in the thermal properties of PHA copolymer. The understanding on thermal properties of PHA is useful to fine tune its molecular morphology during processing.

ACKNOWLEDGEMENTS

This project was financially supported in parts by the Ministry of Higher Education (MOHE, Malaysia) for the LRGS grant (Kenaf: Sustainable Materials in Automotive Industry), Research Excellent Fund from Universiti Teknologi MARA [600-RMI/DANA 5/3/RIF (636/2012)] and Internal Grant of Postgraduate Research Fund (UM.TNC2/IPPP/UPGP/638/PPP).

REFERENCES

- Doi Y, Kanesawa Y, Kunioka M. Biodegradation of Microbial Copolyesters: Poly(3-hydroxybutyrate-co-3-hydroxyvalerate) and Poly(3-hydroxybutyrate-co-4-hydroxybutyrate). *Macromol* 1990;23 :26-31.
- Mergaert J, Anderson C, Wouters A, Swings J, Kersters K. Biodegradation of Polyhydroxyalkanoates, *FEMS Microbiol Rev* 1992;2-4 :317-21.
- Luo L, Wei X, Chen GQ. Physical Properties and Biocompatibility of Poly(3-hydroxybutyrate-co-3-hydroxyhexanoate) Blended with Poly(3-hydroxybutyrate-co-4-hydroxybutyrate). *J Biomater Sci Polym Ed* 2009;20 :1537-53.
- Cheng ST, Chen ZF, Chen GQ. The Expression of Cross-linked Elastin by Rabbit Blood Vessel Smooth Muscle Cells Cultured in Polyhydroxyalkanoate Scaffolds. *Biomater* 2008;29 :4187-94.
- Barham PJ, Keller A, Otun EL, Holmes PA. Crystallization and Morphology of a Bacterial Thermoplastic: Poly-3-hydroxybutyrate. *J Mater Sci* 1984;19 :2781-94.
- Kopinke FD, Remmler M, Mackenzie K. Thermal Decomposition of Biodegradable Polyesters-I: Poly(β -hydroxybutyric acid). *Polym Degrad Stab* 1996;52 :25-38.
- Li SD, He JD, Yu PH, Cheung MK. Thermal Degradation of Poly(3-hydroxybutyrate) and Poly(3-hydroxybutyrate-co-3-hydroxyvalerate) as Studied by TG, TG-FTIR and Py-GC/MS. *J Appl Polym Sci* 2003;89 :1530-36.
- Wong YM, Brigham CJ, Rha C, Sinskey AJ, Sudesh K. Biosynthesis and Characterization of Polyhydroxyalkanoate Containing High 3-hydroxyhexanoate Monomer Fraction from Crude Palm Kernel Oil by Recombinant *Cupriavidus necator*. *Bioresour Technol* 2012;121 :320-27.
- Budde CF, Riedel SL, Willis LB, Rha C, Sinskey AJ. Production of Poly(3-hydroxybutyrate-co-3-hydroxyhexanoate) from Plant Oil by Engineered *Ralstonia eutropha* Strains. *Appl Environ Microbiol* 2011;77 :2847-54.
- Wang Y, Bian Y, Wu Q, Chen GQ. Evaluation of Three-dimensional Scaffolds Prepared from Poly(3-hydroxybutyrate-co-3-hydroxyhexanoate) for Growth of Allogeneic Chondrocytes for Cartilage Repair in Rabbits. *Biomater* 2008;29 :2858-68.
- Wang YW, Yang F, Wu Q, Chen YC, Yu PHF, Chen J, et al. Effect of Composition of Poly(3-hydroxybutyrate-co-3-hydroxyhexanoate) on Growth of Fibroblast and Osteoblast. *Biomater* 2005;26 :755-61.
- Rossi S, Azghani AO, Omri A. Antimicrobial Efficacy of a New Antibiotic-loaded Poly(hydroxybutyric-co-hydroxyvaleric Acid) Controlled Release System. *J Antimicrob Chemother* 2004;54 :1013-18.
- Shishatskaya EI, Gerova AV, Voinova ON, Inzhevatin EV, Khlebopros RG, Volova TG. Evaluation of Antitumor Activity of Rubomycin Deposited in Absorbable Polymeric Microparticles. *Bull Exp Biol Med* 2008;145 :358-61.
- Yao YC, Zhan XY, Zhang J, Zou XH, Wang ZH, Xiong YC, et al. A Specific Drug Targeting System Based on Polyhydroxyalkanoate Granule Binding Protein PhaP Fused with Targeted Cell Ligands. *Biomater* 2008;29 :4823-30.
- Avrami M. Kinetics of Phase Change. I. General Theory. *J Chem Phys* 1939;7 :1103-13.
- Chen C, Cheung MK, Yu PH. Crystallization Kinetics and Melting Behaviour of Microbial Poly(3-hydroxybutyrate-co-3-hydroxyhexanoate). *Polym Int* 2005;54 :1055-64.
- Cai H, Qiu Z. Effect of Comonomer Content on the Crystallization Kinetics and Morphology of Biodegradable Poly(3-hydroxybutyrate-co-3-hydroxyhexanoate). *Phys Chem Chem Phys* 2009;11 :9569-77.
- Ye HM, Wang Z, Chen GQ, Xu J. Different Thermal Behaviors of Microbial Polyesters Poly(3-hydroxybutyrate-co-3-hydroxyvalerate-co-3-hydroxyhexanoate) and Poly(3-hydroxybutyrate-co-3-hydroxyhexanoate). *Polym* 2010;51 :6037-46.
- Fukui T, Doi Y. Cloning and Analysis of the Poly(3-hydroxybutyrate-co-3-hydroxyhexanoate) Biosynthesis Genes of *Aeromonas caviae*. *J Bacteriol* 1997;179 :4821-30.
- Doi Y, Kitamura S, Abe H. Microbial Synthesis and Characterization of Poly(3-hydroxybutyrate-co-3-hydroxyhexanoate). *Macromol* 1995;28 :4822-28.
- Braunegg G, Sonnleitner B, Lafferty RM. A Rapid Gas Chromatographic Method for the Determination of Poly- β -hydroxybutyric Acid in Microbial Mass. *Eur J Appl Microbiol Biotechnol* 1978;6 :29-37.
- Hoffman JD. Role of Reptation in the Rate of Crystallization of Polyethylene Fractions from the Melt. *Polym* 1982;23 :656-70.
- Lorenzo AT, Arnal ML, Albuerne J, Müller AJ. DSC Isothermal Polymer Crystallization Kinetics Measurements and the Use of the Avrami Equation to Fit the Data: Guidelines to Avoid Common Problems. *Polym Test* 2007;26 : 222-31.
- Hay JN, Mills PJ. The Use of Differential Scanning Calorimetry to Study Polymer Crystallization Kinetics. *Polym* 1982;23 :1380-84.
- Chan CH, Kummerlöwe C, Kammer HW. Crystallization and Melting Behavior of Poly(3-hydroxybutyrate)-Based Blends. *Macromol Chem Phys* 2004;205 :664-75.